J. Fluid Mech. (1970), *vol.* 44, *part* 3, *pp.* 461–479
Printed in Great Britain

On the stability of two-dimensional stagnation flow

By J. KESTIN AND R. T. WOOD
Brown University

(Received 3 July 1969 and in revised form 13 March 1970)

The paper examines the stability of the uniform flow which approaches a two-dimensional stagnation region formed when a cylinder or a two-dimensional blunt body of finite curvature is immersed in a crossflow. It is shown that such a flow is unstable with respect to three-dimensional disturbances. This conclusion is reached on the basis of a mathematical analysis of a simplified form of the disturbance equation for the stream-wise component of the vorticity vector. The ultimate, or stable, flow pattern is governed by a singular Sturm–Liouville problem whose solution possesses a single eigenvalue. The resulting flow is one in which a regularly distributed system of counter-rotating vortices is superimposed on the basic, Hiemenz-like pattern of streamlines. The spacing of the vortices is a unique function of the characteristics of the flow, and a theoretical estimate for it agrees well with experimental results. The analysis is extended heuristically to include the effect of free-stream turbulence on the spacing.

The problem is similar to the classical Görtler–Hämmerlin study of the stability of stagnation flow against an infinite flat plate, which revealed the existence of a spectrum of eigenvalues for the disturbance equation. The present analysis yields the same result when an infinite radius of curvature is assumed for the blunt body.

1. Introduction

It has been suspected for a long time that a uniform flow approaching a two-dimensional stagnation region is inherently unstable. We are thinking here about uniform incompressible flows past cylinders or other two-dimensional blunt bodies placed in crossflow, and hypothesize that random disturbances carried by the free stream cause the flow to become three-dimensional. The purpose of this paper is to confirm this hypothesis and to investigate the nature of the resulting three-dimensional flow pattern when a steady state has set in. This will lead to the assertion that a truly two-dimensional flow field is impossible in the circumstance.

Perhaps the earliest indication that the flow in the stagnation region of a blunt body acquires a complex pattern is contained in two papers by Piercy & Richardson (1928, 1930), who concluded that "[there exists] a considerable area of instability extending upstream a distance about one-quarter of the length of the strut section and roughly covering the area for which the mean velocity is sensibly reduced below its value in the undisturbed stream.... Within the area

explored, velocity amplitude (the amplitude of the usually observed fluctuating component) increases rapidly as the stagnation point is approached". More recent hot-wire measurements by Kuethe, Willmarth & Crocker (1959) disclosed the same behaviour near blunt-nosed bodies of revolution. In all cases, the disturbed area extended over a distance of 30 to 50 boundary-layer thicknesses from the surface.

The second important indication is contained in Görtler's (1940) well-known paper on flows along concave walls, which have been shown to become unstable and to develop a discrete system of counter-rotating vortices whose centres are spaced at fixed distances λ, as measured between two vortices rotating in the same sense. Noting that the streamlines in a two-dimensional stagnation region are concave, Görtler (1955) conjectured that such flows might also become unstable and suspected that they, too, should develop a discrete system of counter-rotating vortices whose wavelength λ, like that along a concave wall, should be fixed by the characteristics of the flow.

In order to analyze the stability of stagnation flow mathematically, Görtler (1955) idealized the problem in the same manner as the corresponding two-dimensional, undisturbed flow problem was idealized by Hiemenz (1911), and derived the disturbance equations for stagnation flow against an infinite flat plate. The equations were, in turn, studied by Hämmerlin (1955), who demonstrated analytically that plane stagnation flow can sustain a three-dimensional disturbance. He showed, in particular, that neutral time-dependent disturbances of the usual kind (i.e. with an amplification exponent $\beta = 0$) can exist for a continuous spectrum of wave-numbers $\alpha = 2\pi(\nu/a)^{\frac{1}{2}}/\lambda$ confined to the range $0 < \alpha^2 < 1$. He further showed numerically that no such disturbances could exist in the interval $1 < \alpha^2 \leqslant 5$ if only exponentially decaying solutions at infinity were admitted. Finally, he was able to prove that the disturbances can amplify if the sum of the amplification factor β, and the square of the wave-number α^2, satisfy the condition $0 < \beta + \alpha^2 < 1$. He did not, however, determine whether such amplified disturbances could exist for $\beta + \alpha^2 \geqslant 1$.

The physical interpretation of this result is that in Hiemenz-type flow there exists an instability for a continuous spectrum of wavelengths. The question as to whether one particular wavelength would become amplified preferentially (i.e. with β reaching a maximum for a given flow condition) remained unanswered.

We take the view that the inconclusive nature of Hämmerlin's investigation is the result of an excessive idealization. In a real situation, we are interested in the characteristics of the flow field which results when a uniform stream, whose velocity at $y \to \infty$ is $V_\infty = \text{const}$, approaches a finite blunt two-dimensional body of finite curvature (radius of curvature R). The most important difference between the Görtler–Hämmerlin investigation and the real case, as the ensuing analysis will confirm, resides in the behaviour of the y-component, $V(y)$, of the velocity of approach. This is illustrated in figure 1, which shows that, in a realistically formulated problem, the velocity $V(y)$ starts out with a linear segment $V \sim y$ in the y-direction, transforming continuously to a constant value, V_∞, as $y \to \infty$. In Hiemenz's idealization, which corresponds to $R \to \infty$, the velocity $V(y)$ remains proportional to y and tends to infinity as $y \to \infty$.

In order to determine the flow pattern which forms ahead of a stagnation line, ideally we would like to trace the formation of the quasi-steady flow observed in a wind tunnel in the presence of random, or at least harmonic, fluctuations in the free stream as the flow starts from rest. This, however, is an impossible task, and the mathematical formulation must concentrate on what we suggest are the

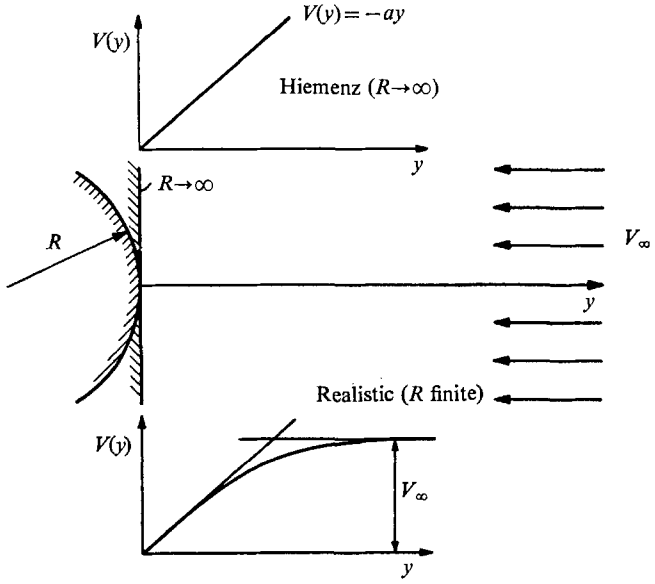

FIGURE 1. Idealized and realistic flow situations compared.

essentials of the problem. In classical analyses of stability problems, a time-dependent disturbance is assumed. For the Hiemenz case, this, as shown by Görtler (1955), can be taken to be of the form,

$$\left.\begin{aligned} u &= [U_0(y) + u_1(y)\cos kz\, e^{\beta t}]\, x, \\ v &= -[V_0(y) + v_1(y)\cos kz\, e^{\beta t}], \\ w &= k w_1(y)\sin kz\, e^{\beta t}, \end{aligned}\right\} \tag{1}$$

for the velocity field $\mathbf{V}(u, v, w)$, and of the form,

$$p = P_0(x, y) + p_1(y)\cos kz\, e^{\beta t} \tag{2}$$

for the pressure field $p(x, y, z)$. Here, k is the disturbance wave-number. In the present analysis we postulate the existence of a steady three-dimensional flow field which is periodic in the z-direction (equation (6) *infra*), and examine whether such a field is compatible with the governing equations and boundary conditions of the motion. In the last analysis, whether a disturbance of the Görtler type is used, or one which is *time*-independent, is a matter of deciding how to attack the problem in hand. In all cases, the basic differential equations are essentially the same. The initial amplitude $e^{\beta t}$ grows to a size sufficient to excite non-linear interactions between the disturbance components; these interactions then retard the growth of the disturbance amplitude until, finally, a steady state,

characterized by some amplitude A, sets in. The analysis given here concentrates on this ultimate state.

Departing from the work of Görtler and Hämmerlin, we develop the relevant flow equations retaining the natural length scale imposed on the problem by the finite dimension of the cylinder cross-section (or curvature of the blunt body). We assume that the oncoming flow, while basically two-dimensional, has superimposed on it a three-dimensional, sinusoidal velocity perturbation in the span-wise direction and require the perturbation amplitude to be vanishingly small in the free stream. The resulting disturbance equations, linearized on the assumption of small perturbations in the usual fashion, yield a singular Sturm–Liouville eigenvalue problem when proper account is taken of the asymptotic nature of the real mean flow at infinity. Subsequently, we show that the theory for this type of eigenvalue problem predicts the existence of a disturbance of unique wavelength, and compare an estimate for this wavelength with direct experimental findings. This comparison goes a little beyond the scope of the theory, in that effects of free-stream turbulence on the flow pattern are discussed in the light of the new understanding provided by the theory. Finally, utilizing a result from the so-called vortex-stretching theory (Sutera, Maeder & Kestin 1963), we supply a qualitative picture of the three-dimensional flow field.

2. Governing equations

As outlined in §1, the mathematical situation we wish to investigate is the steady flow of a viscous, incompressible fluid of constant properties in the neighbourhood of the forward stagnation line on a circular cylinder (or blunt body with radius of curvature R) placed normal to a uniform stream. The oncoming flow, while basically two-dimensional, has superimposed on it a three-dimensional, sinusoidal velocity perturbation whose amplitude is vanishingly small in the free

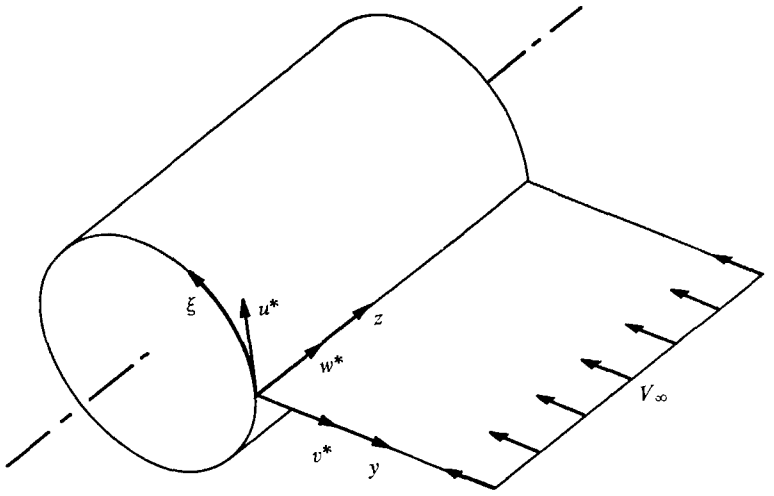

FIGURE 2. Flow geometry for circular cylinder.

stream. Our immediate goal is to determine the wavelengths of those disturbances (if any) which the flow can sustain.

The co-ordinate system $\mathbf{r}(\xi, y, z)$ adopted for this study is shown in figure 2: ξ, y and z represent the tangential, normal and span-wise co-ordinates, respectively. In dimensional notation (now denoted by an asterisk superscript), the flow field is specified by the velocity $\mathbf{V}^* = (u^*, v^*, w^*)$ and the pressure $p^*(\xi, y, z)$. The fluid properties of interest are the density, $\rho = \text{const}$, and the kinematic viscosity, $\nu = \text{const}$, and the fundamental equations describing the flow are:

continuity,
$$\nabla . \mathbf{V}^* = 0, \tag{3}$$

and

momentum,
$$(\mathbf{V}^* . \nabla)\, \mathbf{V}^* = -\frac{1}{\rho} \nabla p^* + \nu \nabla^2 \mathbf{V}^*. \tag{4}$$

These equations are subject to the boundary conditions,

$y = 0$ (wall),
$$\mathbf{V}^*(\xi, 0, z) = 0 \tag{5a}$$

$y \to \infty$ (free stream),
$$u^* \to 0, \quad v^* \to -V_\infty, \quad w^* \to 0. \tag{5b}$$

3. Assumed form of solution

Solutions to the above equations are investigated only in a narrow wedge-shaped domain (see figure 3) encompassing the stagnation plane σ. Strictly speaking, it will be necessary to show that the solution of the differential equations which are simplified by virtue of this restriction are asymptotically the same as the solutions of the full equations in the same region. In making this restriction, we assume that the resulting equations represent an acceptable approximation to the actual flow. If this is granted, it is realized that the same similarity as that used by Hiemenz continues to apply. Thus, we assume the following form of the solution:

$$\left.\begin{aligned} u^* &= [U_0(y) + u_1^*(y) \cos kz]\, \xi, \\ v^* &= -[V_0(y) + v_1^*(y) \cos kz], \\ w^* &= (1/k)\, w_1^*(y) \sin kz, \\ p^* &= P_0(\xi, y) + p_1^*(y) \cos kz. \end{aligned}\right\} \tag{6}$$

Here, the subscript 0 refers to the mean (unperturbed) flow, whereas the subscript 1 refers to the superimposed disturbance. The fundamental wave-number of the periodic secondary motion is k. It must be emphasized that the mean flow components $U_0(y)$ and $V_0(y)$ assumed here must be conceived as functions which are different from those in Hiemenz's solution, because the asymptotic behaviour of $V_0(y)$ as $y \to \infty$ is different; this was explained earlier in conjunction with figure 1.

An examination of the basic flow equations (3) and (4) in the light of the assumed form of solution (6) reveals that it is advantageous to introduce the vorticity $\boldsymbol{\omega}^* = (\omega_\xi^*, \omega_y^*, \omega_z^*)$ and to treat its ξ-component, ω_ξ^*, as an additional unknown. By definition, the vorticity is

$$2\boldsymbol{\omega}^* = \nabla \times \mathbf{V}^*, \tag{7}$$

giving, from the assumed solution (6),

$$2\omega_\xi^* = 2\omega_1^*(y)\sin kz, \tag{8}$$

where

$$2\omega_1^*(y) = \frac{1}{k}\frac{dw_1^*}{dy} - kv_1^*(y). \tag{8a}$$

Replacing the z-component of the momentum equation (4) with the ξ-component of the vorticity-transport equation,

$$(\mathbf{V}^*.\nabla)\,\boldsymbol{\omega}^* = (\boldsymbol{\omega}^*.\nabla)\,\mathbf{V}^* + \nu\nabla^2\boldsymbol{\omega}^*, \tag{9}$$

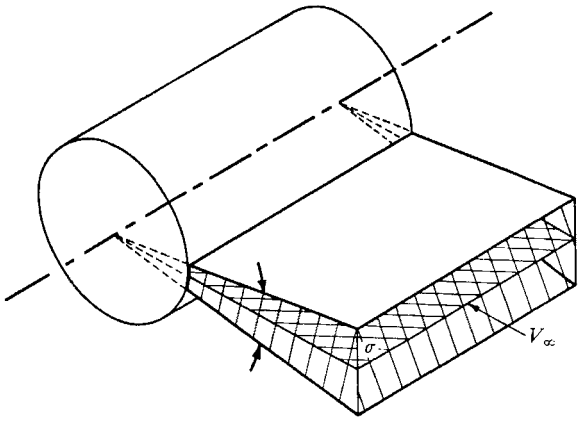

FIGURE 3. Narrow wedge-shaped domain encompassing stagnation plane σ.

we can eliminate the velocity w_1^* in favour of the vorticity perturbation ω_1^*. This procedure also eliminates the pressure perturbation p_1^* and results in simpler equations than those which would be obtained by the straightforward elimination of p_1^* from (3) and (4).

4. Linearized disturbance equations

The working equations for the analysis are obtained by substituting the assumed solution (6) and the computed vorticity (8) into the continuity equation (3), the ξ- and y-components of the momentum equation (4) and the ξ-component of the vorticity transport equation (9).

Neglecting the products of the disturbance quantities we obtain a set of equations which is sufficient to determine the velocity field and the unperturbed pressure field. If desired, the perturbed pressure field can be computed subsequently with the aid of the z-component of the momentum equation (4).

Approximations for the differential operations involving the ∇-operators are employed to evaluate equations (3), (4) and (9) within the narrow region shown in figure 3. These approximations are readily derived from the well-known formulae for differential operations in a system of cylindrical co-ordinates (r, θ, z) by setting $r = R+y$, $\theta = \xi/R$ and $z = z$. Thus, the radial co-ordinate r is replaced by the normal co-ordinate y, measured from the surface; the azimuthal

co-ordinate θ is replaced by the tangential co-ordinate ξ/R (R is the radius of the cylinder); and it is assumed that $\xi/R \ll 1$.

When the above steps are followed, the continuity equation (3) separates into the equations:

$$U_0(y) - \frac{d}{dy}\left[\left(1+\frac{y}{R}\right)V_0\right] = 0, \tag{10a}$$

and

$$u_1^*(y) - \frac{d}{dy}\left[\left(1+\frac{y}{R}\right)v_1^*\right] + \left(1+\frac{y}{R}\right)w_1^*(y) = 0. \tag{10b}$$

The left-hand side of the first equation comprises terms which are independent of the co-ordinate z, whereas the left-hand side of the second equation is the coefficient of $\sin kz$. In order to satisfy the full equation (3), each group of terms must vanish individually. Continuing in like manner, we separate the remaining equations into two parts: a set of equations for the mean-flow variables U_0, V_0, P_0, and a set of equations for the disturbed-flow variables u_1^*, v_1^*, ω_1^* (w_1^* and p_1^* to be eliminated).

The equations are now rendered dimensionless through the introduction of the following variables, which are scaled with respect to the radius R and the free-stream velocity V_∞:

(i) magnified normal co-ordinate:

$$\eta = \frac{y/R}{\epsilon},$$

where

$$\epsilon = Re^{-\frac{1}{2}} = \left(\frac{2V_\infty R}{\nu}\right)^{-\frac{1}{2}};$$

(ii) mean velocity:

$$U = U_0 R/V_\infty, \quad V = \frac{1}{\epsilon}\frac{V_0}{V_\infty};$$

(iii) disturbed velocity:

$$u = u_1^*\frac{R}{V_\infty}, \quad v = \frac{1}{\epsilon}\frac{v_1^*}{V_\infty}, \quad \omega = \omega_1^*\frac{R}{V_\infty};$$

(iv) wave-number:

$$\alpha = \epsilon R k.$$

Finally, we define a new variable,

$$\phi = \frac{1}{2\epsilon}\frac{V_0}{V_\infty}, \tag{11}$$

and eliminate $U_0(y)$ from the equations by means of the mean-flow continuity equation (10a). The function ϕ is the 'cylindrical' counterpart of the Hiemenz function $\phi_H = (a\nu)^{-\frac{1}{2}}V_0$. Since the potential flow about a circular cylinder (Milne-Thomson 1960, p. 151) has the constant

$$a = 2V_\infty/R,$$

it can be shown that ϕ and ϕ_H converge to each other in the boundary layer, so that

$$\phi_H = (a\nu)^{-\frac{1}{2}}V_0 = \left(\frac{R}{2V_\infty\nu}\right)^{\frac{1}{2}}V_0 = \frac{1}{2\epsilon}\frac{V_0}{V_\infty} = \phi \quad (y \to 0).$$

The (linearized) disturbance equations become

$$u''+\left[\phi+\frac{\epsilon}{1+\epsilon\eta}\right]u'-\left[2\phi'+\alpha^2+\epsilon\phi+\frac{\epsilon^2}{(1+\epsilon\eta)^2}\right]u$$
$$=-\left[(1+\epsilon\eta)\,\phi''+\frac{\epsilon^2}{1+\epsilon\eta}\phi+3\epsilon\phi'\right]v, \tag{12}$$

$$v''+\frac{\epsilon}{1+\epsilon\eta}v'-\left[\alpha^2+\frac{\epsilon^2}{(1+\epsilon\eta)^2}\right]v=2\alpha\omega+\left(\frac{u}{1+\epsilon\eta}\right)', \tag{13}$$

$$\omega''+\left[\phi+\frac{\epsilon}{1+\epsilon\eta}\right]\omega'-\left[\alpha^2-\phi'+\frac{\epsilon^2}{(1+\epsilon\eta)^2}\right]\omega=-2\alpha\frac{\epsilon u}{(1+\epsilon\eta)^2}. \tag{14}$$

The equation for u stems from the ξ-momentum equation (4); the equation for v is derived by the elimination of w between (8a) and (10b); and the equation for ω follows from the ξ-vorticity equation (9). In view of the restriction of the equations to a narrow region surrounding the stagnation plane, a term containing $(\xi/R)^2$ was dropped from (14).

An equation for the mean flow (i.e. the function ϕ) is obtained by combining the ξ- and y-components of the momentum equation (4); this also supplies an expression for the mean pressure field in terms of derivatives and integrals of ϕ. The resulting mean-flow equation is

$$(1+\epsilon\eta)\,[\phi^{(\mathrm{iv})}+\phi\phi'''-\phi'\phi'']-2\epsilon[\epsilon^2\phi^2+2\epsilon\phi\phi'+(1+\epsilon\eta)\,\phi'^2-\phi\phi'']$$
$$+\epsilon\left[2\left(\frac{\epsilon}{1+\epsilon\eta}\right)^3\phi-2\left(\frac{\epsilon}{1+\epsilon\eta}\right)^2\phi'+\frac{\epsilon}{1+\epsilon\eta}\phi''+5\phi'''\right]=0. \tag{15}$$

Owing to its complexity, this equation will not be solved; instead, a suitable approximation for ϕ, valid in the wedge under consideration, will suffice for the present study.

The boundary conditions on the above equations derive from the original boundary conditions (5) and are as follows:

$$\eta=0: u=v=v'=0, \quad \phi=\phi'=0; \tag{15a}$$

$$\eta\to\infty: u\to 0, \quad v'\to 0, \quad \phi\to(2\epsilon)^{-1}, \quad \phi'\to 0. \tag{15b}$$

The boundary conditions on ω are implied by (13); their derivation will be postponed temporarily.

In the disturbance equations (12)–(14), the terms multiplied by powers of the scale factor $\epsilon = Re^{-\frac{1}{2}}$ arise as a result of surface curvature. For a typical range of operating Reynolds numbers, say $Re = O(10^5)$, $\epsilon \ll 1$ and the terms involving ϵ can be neglected *provided that this does not destroy the character of the equations* as $\eta\to\infty$. The disturbance equations simplify to read

$$u''+\phi u'-(2\phi'+\alpha^2+\epsilon\phi)\,u=-(1+\epsilon\eta)\,\phi''v, \tag{16}$$

$$v''-\alpha^2 v=2\alpha\omega+\left(\frac{u}{1+\epsilon\eta}\right)', \tag{17}$$

$$\omega''+(\phi\omega)'-a^2\omega=0. \tag{18}$$

Within the boundary layer, ϕ can be represented by the Hiemenz function, because $\epsilon\eta \ll 1$ as well as $\epsilon\phi \ll 1$. Outside the boundary layer, however, the mean-flow function ϕ departs from the Hiemenz solution and becomes asymptotically constant in the free stream. This behaviour, which is a consequence of the body's finite size, significantly affects the eigenvalue problem for the wave-number α.

5. Behaviour of the vorticity ω

Setting $\phi = (2\epsilon)^{-1}$ and $\phi' = 0$ in (18), we obtain the bounded asymptotic $(\eta \to \infty)$ solution,

$$\omega \sim \exp\left\{-\frac{1}{4\epsilon}[1+(1+16\epsilon^2\alpha^2)^{\frac{1}{2}}]\eta\right\} \quad (\alpha \neq 0), \tag{19}$$

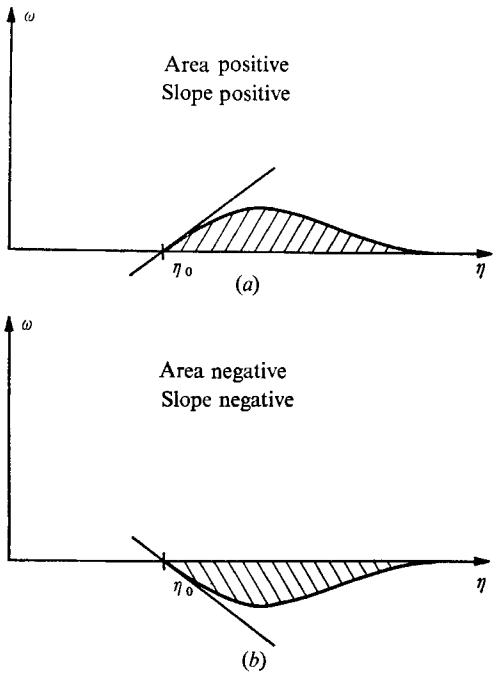

FIGURE 4. Impossible behaviour of vorticity ω in finite-body case. (Area under curve and slope at $\eta = \eta_0$ must have opposite sign.)

(*a*) $\omega(\eta_0) = 0$; $\omega'(\eta_0) > 0$. (*b*) $\omega(\eta_0) = 0$; $\omega'(\eta_0) < 0$.

which satisfies (17) and the conditions (15*b*), i.e.

$$\lim_{\eta\to\infty} \omega'(\eta) = 0. \tag{20}$$

The solution (19) contains the information that

$$\lim_{\eta\to\infty} \omega(\eta) = 0. \tag{21}$$

These results in hand, it can now be demonstrated that, for real wave-numbers ($\alpha^2 > 0$), the function ω has no zeros on the interval $[0,\infty)$. To see this, we

suppose that ω has a number (at least one) of zeros, the greatest of which is η_0, and integrate (18) between η_0 and infinity to obtain

$$-\omega'(\eta_0) = \alpha^2 \int_{\eta_0}^{\infty} \omega(y)\, dy. \tag{22}$$

Under the above assumptions ω must behave as shown in figures 4 (*a*) or 4 (*b*); but both behaviours contradict (22) for $\alpha^2 > 0$, and therefore it follows that ω has only one sign (i.e. no zeros) on the interval $[0, \infty)$ for real values of α. Moreover, since $\phi(0)\,\omega(0) = 0$, (22) holds for $\eta_0 = 0$ and shows that

$$-\omega(0)\,\omega'(0) > 0. \tag{23}$$

With these preliminaries established, the eigenvalue problem can now be examined.

6. The eigenvalue problem

The purpose of § 6 is to investigate the eigenvalue problem posed by (16)–(18), with the boundary conditions (15*a*, *b*), and to discover the nature of the eigenvalue spectrum, i.e. those wavelengths $\alpha > 0$ for which solutions to the equations exist. There is sufficient information available on the boundary conditions and on the behaviour of the vorticity to conclude that the nature of the spectrum is determined solely by the vorticity equation (18). Naturally, the details of the eigenfunctions depend on all of (16)–(18), although no attempt will be made here to solve the complete set.

6.1. *The singular Sturm–Liouville problem*

The substitution,

$$\omega(\eta) = f(\eta) \exp\left[-\frac{1}{2}\int_0^{\eta} \phi(y)\, dy\right], \tag{24}$$

transforms (18) to the canonical form,

$$f'' - (\tfrac{1}{4}\phi^2 - \tfrac{1}{2}\phi' + \alpha^2) f = 0. \tag{25}$$

In view of the inequality (23), the wall boundary condition on f can be expressed as

$$f'(0) + \gamma f(0) = 0, \tag{26}$$

where $\gamma > 0$ is a constant. The exact value of γ is unimportant for the present argument; it must be found from the complete solution to the problem. The asymptotic ($\eta \to \infty$) solution to (25) is

$$f_a \sim \exp\left[-\frac{1}{4\epsilon}(1 + 16\epsilon^2\alpha^2)^{\frac{1}{2}}\, \eta\right]. \tag{27}$$

Equation (25), with its boundary condition (26) and asymptotic behaviour (27), constitutes the familiar and well-treated singular Sturm–Liouville problem. In the present version of this problem, solutions are sought to an equation of the form,

$$f'' + [\mu - q(\eta)] f = 0 \quad (a < \eta < b), \tag{28}$$

with the boundary condition (26), when the interval (a, b) is semi-infinite. The entire problem, and in particular the case of the semi-infinite interval $[0, \infty)$, is treated extensively by Dunford & Schwartz (1963). What follows is a restatement of certain theorems and corollaries which are relevant to equation (25); they reveal the nature of the eigenvalue spectrum.

6·2. *Nature of the entire eigenvalue spectrum*

(i) Let L be a real second-order differential operator of the form

$$\mathsf{L} = -\frac{d^2}{d\eta^2} + q(\eta) \tag{29a}$$

$$q(\eta) = \tfrac{1}{4}\phi^2 - \tfrac{1}{2}\phi', \quad \text{and} \quad \mu = -\alpha^2 \tag{29b,c}$$

(for the moment the restriction $\alpha^2 > 0$ will be dropped and μ will be considered a real number, positive or negative). Then (25) reads:

$$\mathsf{L}[f] = \mu f, \tag{30}$$

with the boundary condition (26) and asymptotic behaviour (27), and the operator is formally self-adjoint. This property, a prerequisite for the current study, is readily established with the aid of an auxiliary function g as follows.

By definition, the operator L is self-adjoint when it equals the adjoint operator L^A given by the inner product expression

$$\int_0^\infty g\mathsf{L}[f]\,d\eta = \int_0^\infty f\mathsf{L}^A[g]\,d\eta. \tag{31a}$$

After integration by parts, the left side of (31a) yields

$$\int_0^\infty g\left[-\frac{d^2}{d\eta^2} + q(\eta)\right] f\,d\eta = \Big[fg' - f'g\Big]_0^\infty + \int_0^\infty f\left[-\frac{d^2}{d\eta^2} + q(\eta)\right] g\,d\eta; \tag{31b}$$

thus, $\mathsf{L} = \mathsf{L}^A$ if the concomitant $[fg' - f'g]_0^\infty = 0$. Since this is possible when g satisfies a boundary condition (26) identical to that on f, the operator is formally self-adjoint.

(ii) (See Dunford & Schwartz 1963, Corollary 56, p. 1481, and theorem 53, p. 1479.) Let the real, formally self-adjoint differential operator L of (30) be defined on the interval $[0, \infty)$, and suppose that

$$\lim_{\eta\to\infty} q(\eta) = \mu_0. \tag{32}$$

Then the spectrum of eigenvalues $\mu \geqslant \mu_0$ is continuous. If

$$\lim_{\eta\to\infty} \eta^2[q(\eta) - \mu_0] < -\tfrac{1}{4}, \tag{33}$$

the remainder $(-\infty, \mu_0)$ of the eigenvalue spectrum consists of an infinite sequence of isolated points converging to μ_0. The isolated points can be enumerated in the ascending sequence $\mu_1 < \mu_2 < \ldots < \mu_p$, with $\mu_p \to \mu_0$ as $p \to \infty$, and with each eigenvalue μ_n there is associated a unique eigenfunction f_n of the operator L. The eigenfunction f_n has precisely $n-1$ zeros.

This result establishes the intimate dependence of the eigenvalue spectrum on the coefficient function $q(\eta)$. All that remains now is to show that the preceding conditions on q are satisfied in the present problem and to restrict the entire spectrum μ to the special case $\mu < 0$ ($\alpha^2 > 0$).

6.3. *The coefficient function* $q(\eta)$

At large distances from the boundary, the mean-flow ϕ is represented by the function

$$\phi_P = \frac{1}{2\epsilon}\left[1 - \frac{1}{(1+\epsilon\eta)^2}\right] \quad (\eta \gg 1), \tag{34}$$

which is obtained by substituting a dimensionless form of the potential-flow solution for a cylinder (Milne-Thomson 1960, p. 151) into (11). Then (29*b*) becomes

$$\lim_{\eta\to\infty} q(\eta) = \frac{1}{16\epsilon^2} = \mu_0, \tag{32a}$$

and

$$\lim_{\eta\to\infty} \eta^2[q(\eta) - \mu_0] = -\frac{1}{8\epsilon^4} < -\tfrac{1}{4} \quad (\epsilon \ll 1); \tag{33a}$$

hence, the conditions of the preceding theorem are met. We now need to determine the behaviour of the function q in the boundary-layer region in order to solve the eigenvalue problem.

Near the boundary, the mean-flow ϕ is the Hiemenz function ϕ_H. When ϕ_H is substituted into (29*b*), the resulting expression for $q(\eta)$ is found to possess a minimum at the point $\eta_{\min}$ given by $q'(\eta_{\min}) = 0$, or

$$\phi_H(\eta_{\min})\,\phi'_H(\eta_{\min}) - \phi''_H(\eta_{\min}) = 0. \tag{35}$$

The Hiemenz function can be approximated to within 10 % by the expression

$$\phi_H = \tfrac{1}{2}\phi''^2_0 - \tfrac{1}{6}\eta^3 \quad (0 \leqslant \eta < 2), \tag{36}$$

which represents the first two terms in the Taylor-series expansion for it. Using the approximation (36), we find that the minimum, $q_{\min}$, of q occurs at

$$\eta_{\min} = s\left\{1 - \frac{2s^4 + s^8}{72 - 28s^4 + 5s^8}\right\}, \tag{37}$$

giving

$$q_{\min} = -\frac{3}{4}\frac{1}{s^2} + \frac{1}{6}s^2, \tag{38}$$

where $s = (2/\phi''_0)^{\frac{1}{3}}$. The Hiemenz solution (Schlichting 1968, p. 87) for the wall shear rate is $\phi''_0 = 1.233$; this leads to $\eta_{\min} = 0{\cdot}94$, equation (37). At this value of η, the approximation (36) is good to 2 % in ϕ_H.

The complete behaviour of the coefficient function $q(\eta)$ is represented by the dashed line $\mu = 0$ in figure 5, which is a sketch (not to scale) of the difference $q(\eta) - \mu$ for several values of μ. This figure graphically displays the connexion between the coefficient function $q(\eta)$ and the entire eigenvalue spectrum, μ, whose nature was described in the previous section. For example, taking the nth eigenvalue, μ_n, we see from figure 5 that $q(\eta) - \mu_n < 0$ for $\eta < \eta_n$. Consequently, in the region $\eta < \eta_n$, the solution to (28) will oscillate, passing through zero precisely

$n-1$ times. On the other hand, all solutions corresponding to eigenvalues $\mu \geqslant \mu_0$ have infinitely many zeros.

6.4. *The restricted spectrum* $\mu < 0$ ($\alpha^2 > 0$)

It follows from the development in § 6.2 (ii) that there exists only one eigenvalue μ_1 to which there corresponds a unique eigenfunction f_1 having no zeros on the

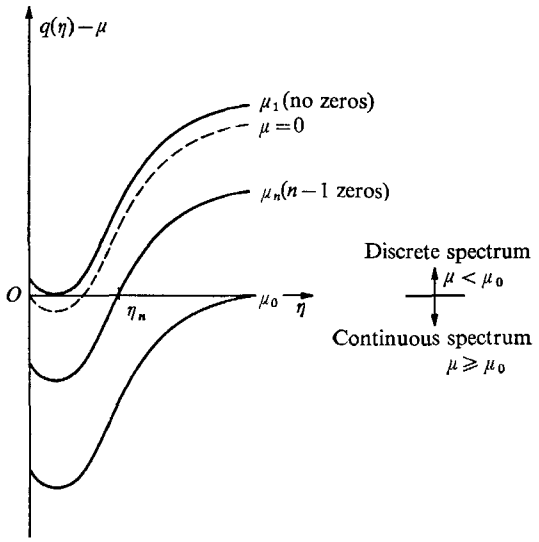

FIGURE 5. The function $q(\eta)-\mu$ for (28); nature of the eigenvalue spectrum μ: $\mu_0 = \lim_{\eta\to\infty} q(\eta)$.

interval $[0, \infty)$. But, as shown in § 5, the vorticity ω (and, consequently, the function f defined by (24)) cannot have zeros on the interval $[0, \infty)$ for real wavenumbers, and therefore the restricted spectrum $\alpha^2 > 0$ can contain only one wavenumber,

$$\alpha^2 = -\mu_1 > 0, \tag{39}$$

if the problem is to possess a solution.

Recalling (28), it becomes evident that a sufficient (but not necessary) condition for the solution f not to have zeros is

$$q(\eta)-\mu > 0 \quad (\text{all } \eta); \tag{40a}$$

otherwise, if $q(\eta)-\mu < 0$ over a range of η, the solution might oscillate (but not necessarily). Thus, (40*a*) sets the limiting condition

$$q_{\min}-\mu_1 = 0 \tag{40b}$$

evidenced in figure 5.

7. Estimate for the disturbance wavelength

The combination of (38), (39) and (40*b*) provides us with the estimate

$$\alpha^2 = -q_{\min} = \frac{3}{4}\left(\frac{\phi_0''}{2}\right)^{\frac{2}{3}} - \frac{1}{6}\left(\frac{2}{\phi_0''}\right)^{\frac{2}{3}}, \tag{41}$$

giving a disturbance wavelength

$$\lambda = \frac{2\pi}{k} = \frac{2\pi R}{\alpha Re^{\frac{1}{2}}}, \tag{41a}$$

or

$$\lambda = \lambda_0 \frac{2^{\frac{4}{3}}}{\phi_0''^{\frac{1}{3}}} \frac{1}{\{3 - (\frac{2}{3})\,[2/\phi_0'']^{\frac{4}{3}}\}^{\frac{1}{2}}}, \tag{41b}$$

where $\lambda_0 = 2\pi R/Re^{\frac{1}{2}}$ is the neutral wavelength defined in the vorticity-amplification theory (Sutera *et al.* 1963), and introduced here for convenience. Incorporating the Hiemenz solution $\phi_0'' = 1{\cdot}233$ in our estimate (41*b*), we find the numerical result that the unique disturbance wavelength

$$\lambda = 1{\cdot}79\lambda_0 = 1{\cdot}79(2\pi R/Re^{\frac{1}{2}}). \tag{41c}$$

The physical interpretation of the preceding results is that two-dimensional stagnation flow against a two-dimensional blunt model is inherently unstable. Even though the solid body is two-dimensional, the flow itself becomes three-dimensional in that it curls up into a system of counter-rotating vortices distributed with a unique wavelength in the z-direction. Owing to the assumption expressed in the boundary conditions (15*b*), the onset of such an instability must be expected to occur even in the limiting case of a vanishing disturbance at $y \to \infty$. Experimentally, this would correspond to a turbulence-free oncoming stream. Furthermore, as the Reynolds number Re is reduced, the spacing λ becomes large and, ultimately, unobservable.

8. The case when $R \to \infty$

It would be interesting at this point to re-examine our stability argument, and to clarify the way in which it changes in the asymptotic limit when the radius of curvature $R \to \infty$. In this limit, our problem would become identical with that studied by Hämmerlin (i.e. with an investigation of the stability of Hiemenz's flow). This has been done, but we find that a detailed account would become tedious for the reader. Instead, it may be sufficient to give a short account of the principal result.

The essential difference between the two cases resides in the assumed asymptotic behaviour of the function $\phi(\eta)$. If $\phi(\eta)$ were to be unbounded, the asymptotic solution ($\eta \to \infty$) for the function f in (25) would also become unbounded; the vorticity ω could acquire at least one zero; and the operator L, defined in (29*a*), would cease to be formally self-adjoint. As a result, the unique eigenvalue, α from (39), would cease to exist, and would be replaced by a continuous spectrum $0 < \alpha^2 < 1$. This, as the reader recalls, is essentially the same result as the one obtained by Hämmerlin.

9. Experimental results

Utilizing the results from a series of wind-tunnel tests described elsewhere (Kestin & Wood 1969), we have secured experimental confirmation for our estimate of the unique disturbance wavelength. Our experiments consisted of flow

visualization studies, which were performed with the aid of oil-coated cylinders of different diameters placed in cross flows of various free-stream velocities (Reynolds numbers) and turbulence levels. After a relatively short exposure to the stream, the oil film on the surface of each cylinder was parted by the flow into a pattern of regularly spaced radial streaks like those shown in figure 6 (plate 1) for a set of representative conditions. The pitch of the streaks was found to correlate well as a function of both Reynolds number and turbulence intensity, and the correlation is represented in figure 7. This demonstrates that the spacing, normalized with respect to the cylinder diameter D, is inversely proportional to $Re^{\frac{1}{2}}$, where the factor of proportionality decreases with increasing turbulence intensity.

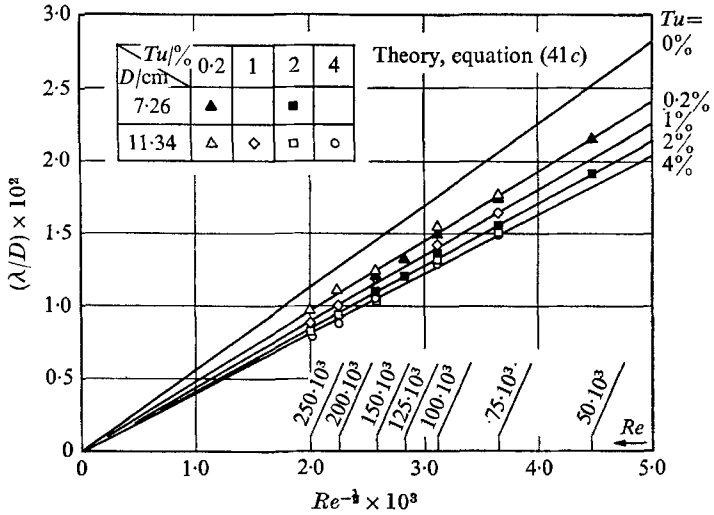

FIGURE 7. Measurements for the dimensionless wavelength λ/D.

In order to interpret these results, it is necessary to realize that the wall shear stress computed from the three-dimensional velocity field (6) consists of an undisturbed value plus a component which is periodic in the axial direction. Thus, since the wall shear stress is responsible for parting the oil film, it becomes evident that the observed streak spacing is identical with the wavelength λ of the three-dimensional instability. Hence, taking into account the remarks made in §7, we extrapolate the measured spacings to the limit of zero turbulence intensity, and obtain the result that $\lambda/\lambda_0 = 1{\cdot}56$ ($Tu \to 0$). This value is appropriate for comparison with our analytical estimate ($\lambda/\lambda_0 = 1{\cdot}79$) derived earlier; the relatively good agreement (14 %) between experiment and theory thus confirms the stability analysis. If, instead of the approximation (36), the tabulated numerical solution for the Hiemenz function (Schlichting 1968, p. 90) were used in the evaluation (35), the estimate would become $\lambda/\lambda_0 = 1{\cdot}72$, which is only 10 % above the experimental value.

The preceding results show that the experiments extrapolate to the analysis. We now demonstrate that, at least qualitatively, the theory can be extended to predict the observed wavelength at non-zero turbulence levels. The demonstration

turns on the experimental measurements of Smith & Kuethe (1966), which reveal that the wall-shear rate ϕ_0'' is an increasing function of the turbulence intensity. Hence, putting $\phi_0'' = \phi_0''(Tu)$ in (41*b*), we conclude that an increase in turbulence intensity will cause a decrease in wavelength (at constant Reynolds number), if we accept heuristically that the form of equation (41*b*) remains valid for turbulent free streams. A feeling for the qualitative validity of this extension can be gained from the following example. At a free-stream turbulence level of 6%, Smith & Kuethe (1966) measured a rate of wall shear at the stagnation line of a circular cylinder in cross flow that was increased by 50% over its low-turbulence value. From (41*b*), the wavelength corresponding to such an increase in ϕ_0'' is $\lambda/\lambda_0 = 1{\cdot}37$ ($Tu = 6\%$); this compares favourably with the result $\lambda/\lambda_0 = 1{\cdot}27$ determined by extrapolating our measured streak spacings to $Tu = 6\%$.

Flow pattern

In order to obtain a picture of the three-dimensional flow field without solving the disturbance equations (16)–(18) for their eigenfunctions, we refer to an existing analysis. This is the so-called vorticity amplification theory (Sutera, Maeder & Kestin 1963; Sutera 1965), which succeeded in determining the flow pattern in a Hiemenz-type boundary layer when a periodic, harmonic disturbance, of given wavelength λ, has been imposed on the free stream in the z-direction. Such a disturbance is equivalent to a continuously distributed vorticity characterized by axes which are aligned in the x-direction, and which are susceptible to stretching and amplification by the divergent streamlines in a stagnation flow.

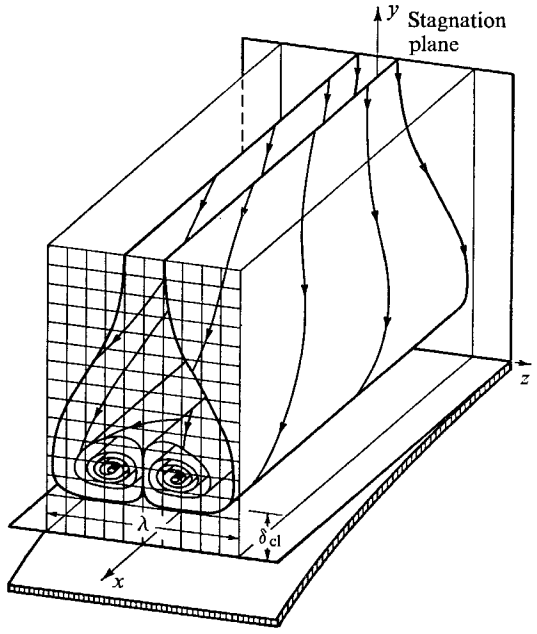

FIGURE 8. Three-dimensional flow pattern deduced with the aid of the vorticity-amplification theory.

This solution can be utilized to provide a qualitative representation of the three-dimensional flow pattern which results from the instability discussed earlier, because the latter also imposes a harmonic disturbance of a fixed wavelength on the approaching flow.

Figures 8, 9 and 10 depict the streamlines of this kind of flow field. Using the method of isoclines, we have traced the streamlines from a numerical solution provided by Williams (1968) for a disturbance of an (arbitrary) amplitude $A = 3$ and an imposed wavelength $\lambda/\lambda_0 = 1{\cdot}67$. Figure 8 is a dimetric drawing of two

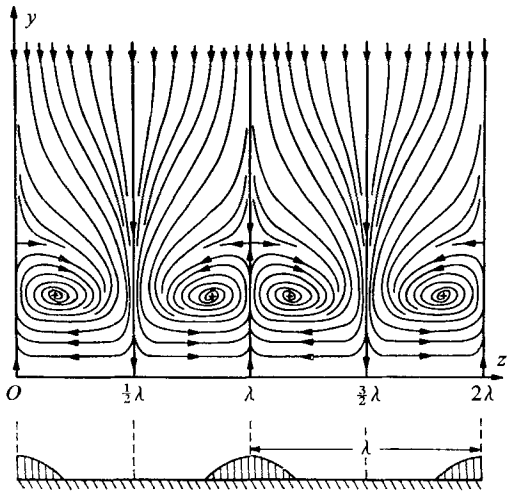

FIGURE 9. Projection of the flow pattern on the stagnation plane.

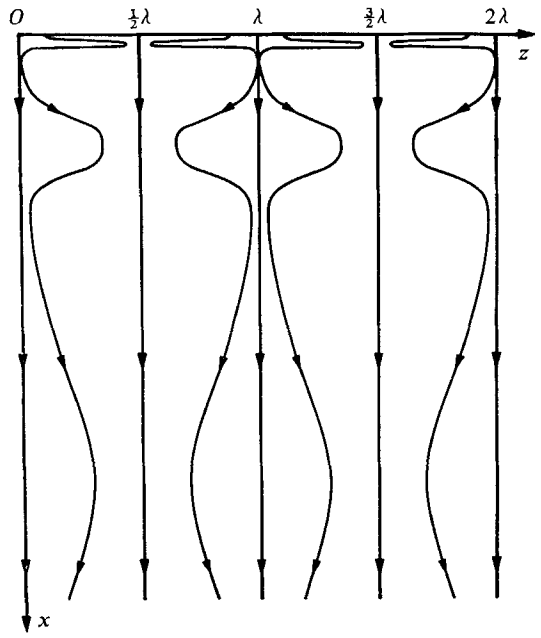

FIGURE 10. Projection of four representative streamlines on the body-tangent plane (x-scale compressed).

symmetric stream surfaces, each containing four representative streamlines. Figure 9 is a projection of the flow pattern on the stagnation y, z-plane (this sketch contains additional streamlines not shown in figure 8). Figure 10 depicts the projection of four streamlines, one contained in each of the four neighbouring cells from figure 9, on the body-tangent x, z-plane.

The nature of the three-dimensional flow is now apparent: the flow pattern consists of stationary, span-wise repetitive cells of width λ equal to the instability wavelength. Each cell contains two cores of concentrated vorticity, which are formed by the rolling-up of concentric stream surfaces. The cores are located slightly outside the edge of the classical (Hiemenz) boundary layer δ_{cl}, and extend transversely across the stagnation line. The streamlines of the flow are wrapped around the cores in helix-like spirals, the pitch of the spirals increasing with increasing distance away from the stagnation line.

A striking experimental confirmation of the preceding behaviour of the flow is provided by the previously unexplained smoke visualization pictures taken by Sadeh (1968). In this study, smoke was injected near the boundary layer in the stagnation flow over a plate of finite width and the resulting flow pattern was photographed. The photographs shown in figure 11 (plate 2) suggest that the streamlines of the disturbed flow do, indeed, form helix-like spirals.

The preceding flow pattern is also consistent with our flow visualization studies (see figure 6, plate 1), with the ablation studies reported by Brun, Diep & Kestin (1966), and with the experimental work described by Kayalar (1969).

We wish to thank Dr Willy Z. Sadeh, formerly of the Division of Engineering, Brown University, for generously allowing us to use his smoke photographs.

The present work was supported in part by the Aerospace Research Laboratories, United States Air Force, Wright–Patterson Air Force Base, Ohio (Contracts AF 33(615)–1263 and F 33(615) 67 C 1754), under the technical supervision of Dr Max Scherberg. Dr Scherberg drew our attention to several instances of flows which become unstable by developing patterns of counter-rotating vortices and recognized their importance in stagnation flows at an early date. This support, together with additional funds from the National Science Foundation (Grant GK-575) and from the Brown University Division of Engineering, is gratefully acknowledged.

Computer time was provided by NSF Grant GP-4825.

REFERENCES

Brun, E. A., Diep, G. B. & Kestin, J. 1966 Sur un nouveau type des tourbillons longitudinaux dans l'écoulement autour d'un cylindre. Influence de l'angle d'attaque et de la turbulence du courant libre. *C.R. Acad. Sci.* **263**, 742.

Dunford, N. & Schwartz, J. T. 1963 *Linear Operators, Part II: Spectral Theory*. New York: Interscience.

Görtler, H. 1940 Über eine dreidimensionale Instabilität laminarer Grenzschichten an konkaven Wänden. *Nachr. Wiss. Ges. Gottingen, Math. Phys. Klasse*, N.F. **2**, 1.

Görtler, H. 1955 Dreidimensionale Instabilität der ebenen Staupunktströmung gegenüber wirbelartigen Strömungen. *Fünfzig Jahre Grenzschichtforschung* (ed. H. Görtler & W. Tollmien). Braunschweig: Vieweg.

HÄMMERLIN, G. 1955 Zur Instabilitätstheorie der ebenen Staupunktströmung. *Fünfzig Jahre Grenzschichtforschung* (ed. H. Görtler & W. Tollmien). Braunschweig: Vieweg.

HIEMENZ, K. 1911 Die Grenzschicht an einem in den gleichförmigen Flüssikeitsstrom eingetauchten geraden Kreisszylinder. *Dingl. Polytech. J.* **326**, 321.

KAYALAR, L. 1969 Experimentalle und theoretische Untersuchungen über den Einfluss des Turbulenzgrades auf den Wärmeübergang in der Umgebung des Staupunktes eines Kreiszylinders. *Forschung a.d. Gebiete des Ingenieurwesens*, **35**, 157.

KESTIN, J. & WOOD, R. T. 1969 Enhancement of stagnation-line heat transfer by turbulence. *Progress in Heat Transfer*, vol. 2, p. 249.

KUETHE, A. M., WILLMARTH, W. W. & CROCKER, G. H. 1959 Stagnation-point fluctuations on a body of revolution. *Phys. Fluids*, **2**, 714.

MILNE-THOMSON, L. M. 1960 *Theoretical Hydrodynamics* (4th ed.). New York: Macmillan.

PIERCY, N. A. V. & RICHARDSON, E. G. 1928 The variation of velocity amplitude close to the surface of a cylinder moving through a viscous fluid. *Phil. Mag.* **6**, 970.

PIERCY, N. A. V. & RICHARDSON, E. G. 1930 The turbulence in front of a body moving through a viscous fluid. *Phil. Mag.* **9**, 1038.

SADEH, W. Z. 1968 An investigation of vorticity amplification in stagnation flow. Ph.D. Thesis, Brown University.

SCHLICHTING, H. 1968 *Boundary-Layer Theory* (6th ed., trans. J. Kestin). New York: McGraw-Hill.

SMITH, M. C. & KUETHE, A. M. 1966 Effects of turbulence on laminar skin friction and heat transfer. *Phys. Fluids*, **9**, 2337.

SUTERA, S. P., MAEDER, P. F. & KESTIN, J. 1963 On the sensitivity of heat transfer in the stagnation-point boundary layer to free-stream vorticity. *J. Fluid Mech.* **16**, 497.

SUTERA, S. P. 1965 Vorticity amplification in stagnation-point flow and its effect on heat transfer. *J. Fluid Mech.* **21**, 513.

WILLIAMS, G. 1968 Enhancement of heat and mass transfer in a stagnation region by free stream vorticity. M.S. Thesis, Brown University.

Note added in proof. Additional information regarding the experimental work mentioned in this paper can be found in the following two references:

KESTIN, J. & WOOD, R. T. 1970*a* The influence of turbulence on mass transfer from cylinders. *ASME Paper* no. 70-WA/HT-3.

KESTIN, J. & WOOD, R. T. 1970*b* The mechanism which causes free stream turbulence to enhance stagnation-line heat and mass transfer. *Heat Transfer* 1970, *Fourth Int.Heat Transfer Conference*, vol. II, paper FC 2.7.

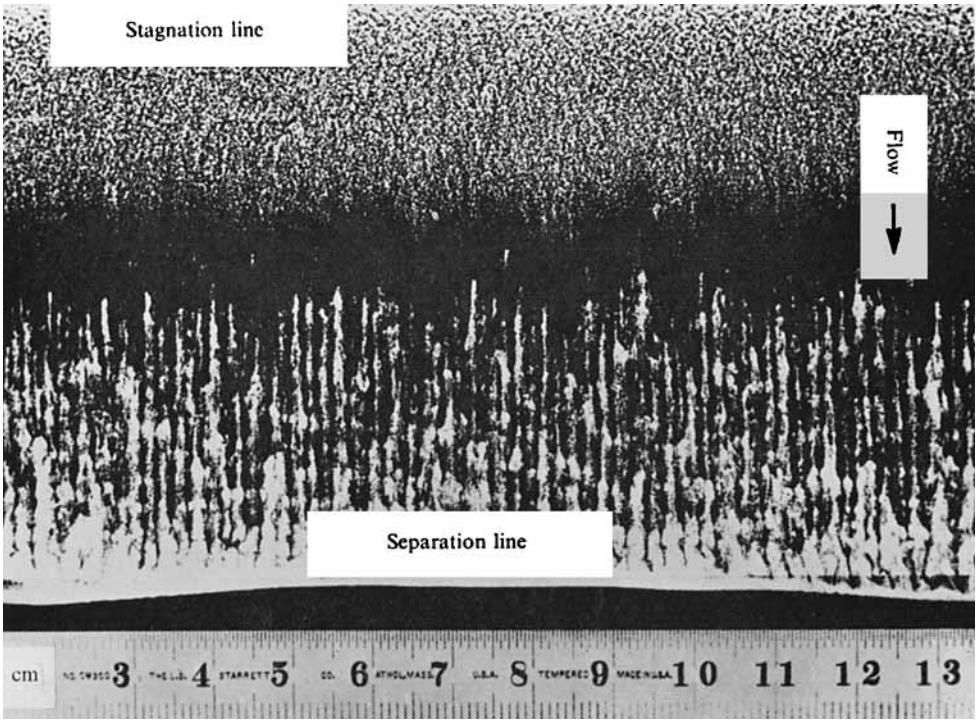

FIGURE 6. Streak pattern for the conditions $Re = 75{,}000$; $Tu = 1{\cdot}2\%$; $D = 11{\cdot}3$ cm.

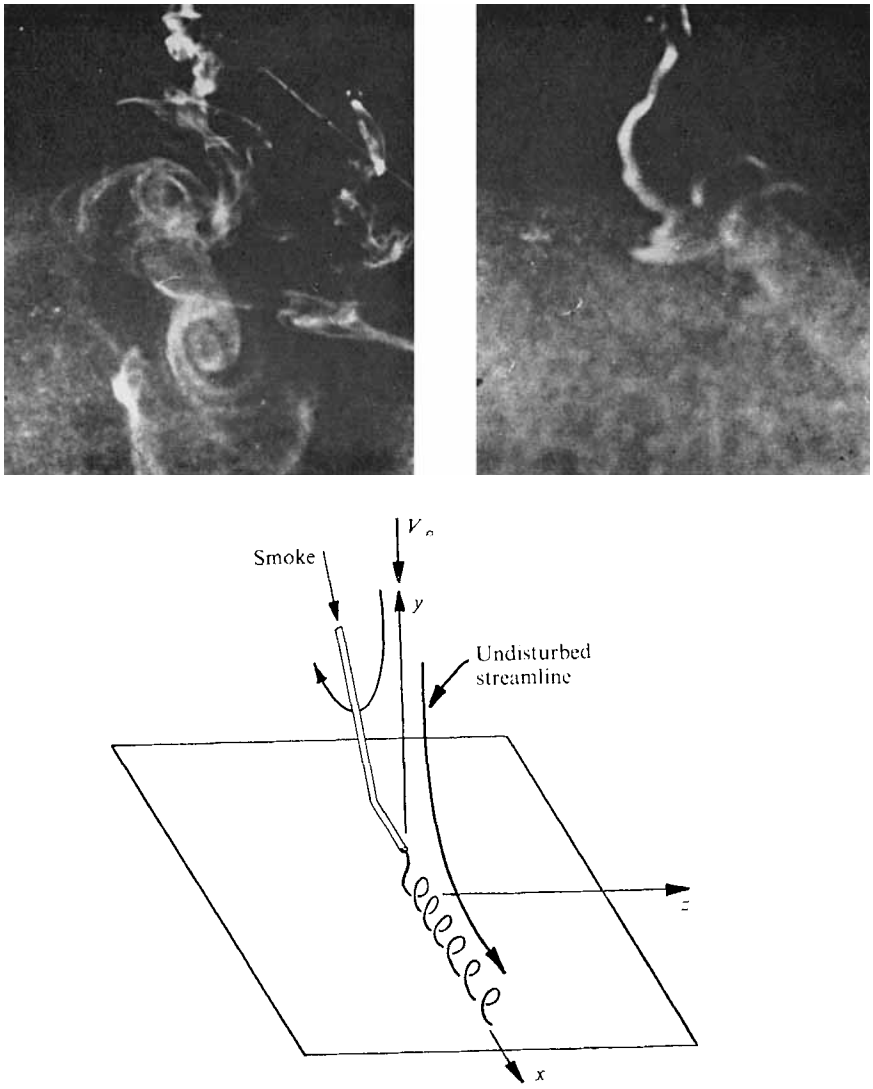

FIGURE 11. Smoke visualization photographs of flow pattern (Sadeh 1968).